THE ASTROPHYSICAL JOURNAL, 459:278–287, 1996 March 1

OPENING A NEW WINDOW ON Ap STAR ATMOSPHERES: A T-τ RELATION FOR HR 3831 FROM ITS LIMB-DARKENED PULSATION AMPLITUDES

JAYMIE M. MATTHEWS[1]
Department of Geophysics and Astronomy, University of British Columbia, Vancouver, BC V6T 1Z4, Canada; matthews@astro.ubc.ca
WILLIAM H. WEHLAU[1,2]
Department of Astronomy, University of Western Ontario, London, Ontario N6A 3K7, Canada
JOHN RICE[1]
Department of Physics and Astronomy, Brandon University, Brandon, Manitoba R7A 6A9, Canada; rice@mickey.brandonu.ca
AND
GORDON A. H. WALKER
Department of Geophysics and Astronomy, University of British Columbia, Vancouver, BC V6T 1Z4, Canada; walker@astro.ubc.ca
Received 1995 July 10; accepted 1995 September 5

ABSTRACT

We demonstrate a new approach for probing the atmospheres of selected chemically peculiar magnetic stars. Using the Cerro Tololo Inter-American Observatory (CTIO) 1.0 and 1.5 m telescopes simultaneously on two nights in 1991, we obtained optical and infrared high-speed photometry of the rapidly oscillating Ap (roAp) star HR 3831 (=HD 83368), which pulsates with a period of ~11.8 minutes. Oscillation amplitudes (or upper limits) in each of eight bandpasses were measured by Fourier analysis, revealing the very steep decline in amplitude with increasing wavelength characteristic of roAp stars. Matthews and coworkers have shown that this can be explained by the wavelength dependence of limb darkening and its filtering effect on the integrated amplitude of an $(l, m) = (1, 0)$ nonradial pulsation mode. Since the eigenfrequency spectrum of HR 3831 is dominated by just such a dipole mode, it is possible to infer limb-darkening coefficients β_λ for its atmosphere from our amplitude measurements. These coefficients are used to derive a source function through the Eddington-Barber relation, which leads to a relation for temperature versus optical depth in the stellar photosphere.

Our results show that the T-τ_{5000} curve is much steeper for HR 3831 than for the Sun (at least at the rotational phase when the star's magnetic pole dominates the visible hemisphere). We also calculate the gradient $dT/d\tau$ as a function of wavelength to compare with the curve expected for H^- continuous opacity. This type of diagnostic may become a useful tool for checking the predictions of diffusion theory.

Subject headings: stars: atmospheres — stars: individual (HR 3831) — stars: oscillations — stars: peculiar

1. INTRODUCTION

The atmospheric structures of peculiar A–F stars are notoriously difficult to model: line blanketing is severe in the ultraviolet, surface gravities are uncertain, there are strong global magnetic fields, the latest atmosphere codes (e.g., Kurucz 1993) still do not completely allow for the anomalous chemical compositions, and surface abundance inhomogeneities lead to different atmospheric properties as a function of position on the star. The recent work of Adelman et al. (1995) is a good example of the hard-won improvements as well as the remaining theoretical and observational challenges in fitting the flux distributions of Ap stars through spectral synthesis. (See also Muthsam & Stepień 1992 and references therein.)

Another diagnostic of atmospheric properties can be the star's pulsation, especially in the case of high radial overtones whose amplitudes are sensitive to conditions in the upper layers. About two dozen cool peculiar A–F stars are now known to pulsate (Martinez & Kurtz 1995). These rapidly oscillating Ap (roAp) stars have periods of a few minutes, and amplitudes generally less than 0.01 mag and 1 km s^{-1} in light and velocity, respectively. For several of the multiperiodic stars, their eigenfrequency patterns are consistent with nonradial acoustic p-modes of low degree and high overtone (e.g., HR 1217; Kurtz et al. 1989). The modes of roAp star appear to be aligned with the inclined magnetic field axis, producing amplitude modulation and sometimes phase shifts during the rotation period (i.e., Kurtz's (1982) oblique pulsator model). The phasing of the modulation and phase shifts, along with fine-splitting of frequencies in the Fourier domain, suggest that many—if not all—roAp stars are dominated by an $(l, m) = (1, 0)$ dipole mode.

Analysis of the complicated p-mode eigenfrequency patterns and splittings of some roAp stars can already provide information about their evolutionary stage, rotation rate, magnetic field geometry, and internal field strength (see, e.g., Kurtz 1990; Matthews 1993a, b). In this paper, we demonstrate a new way to exploit the pulsations of roAp stars—in particular, those having only one excited dipole mode—to probe their atmospheric structure.

1.1. *Pulsation Amplitudes and Limb Darkening*

For most classical radial pulsars (Cepheids, RR Lyrae, and larger amplitude δ Scuti stars), once the effects of geo-

[1] Visiting Astronomer, Cerro Tololo Inter-American Observatory, National Optical Astronomy Observatories, operated by the Association of Universities for Research in Astronomy, Inc., under contract with the National Science Foundation.

[2] Deceased 1995 January 23. The surviving authors dedicate this paper to the memory of their colleague, Bill Wehlau, whose wisdom and foresight will continue to influence Ap star research for some time to come. This collaboration—and our lives—will be sadly diminished by Bill's absence.

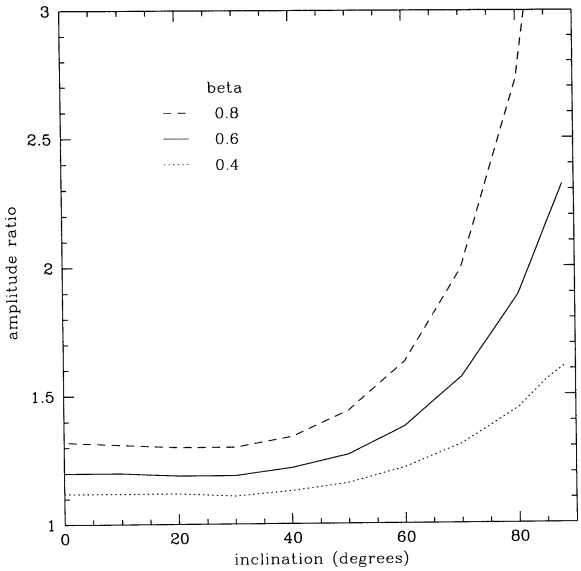

FIG. 1.—Enhancement of the intrinsic pulsation amplitude of an (l, m) = (1, 0) dipole mode as a function of mode inclination, for three amounts of limb darkening expressed by eq. (1). The vertical axis shows the ratio of the calculated amplitudes with and without limb darkening.

metrical variations are removed, the observed relation between flux amplitude and wavelength is consistent with that of a pulsating blackbody source. But the roAp stars deviate significantly from this behavior. Within a few years of the discovery of the class, multicolor photometry (e.g., Weiss & Schneider 1984) had established that roAp pulsation amplitudes decline much more rapidly with increasing wavelength than those of classical pulsating variables.

Matthews, Wehlau, & Walker (1990) showed that this can be explained by the wavelength dependence of limb darkening and its weighting effect on the integrated amplitude of the (l, m) = (1, 0) mode. The dipole has two special features which make this effect so important as a diagnostic: (1) It produces no changes in the surface area of the star during the pulsation cycle, so the observed light oscillations can be attributed totally to flux (i.e., temperature) variations; and (2) no matter what the inclination $i_{\rm puls}$ of the pulsation pole, limb darkening *increases* the net amplitude of a dipole mode integrated over the visible disk.[3]

That stronger limb darkening at shorter wavelengths enhances the effective amplitude is demonstrated by Figure 1, in which the enhancement factor for a dipole mode is shown as a function of the inclination of the pulsation pole for three different levels of limb darkening. The limb darkening has been represented by

$$\frac{I_\lambda(\theta)}{I_\lambda(0)} = 1 - \beta_\lambda(1 - \cos\,\theta)\,, \qquad (1)$$

where β_λ is the limb-darkening coefficient as a function of wavelength and θ is the angle from the subsolar point on the stellar disk. (Note that the curves in Fig. 1 were produced by the model described later on in § 3.1.)

By measuring the oscillation amplitudes of an roAp star at various wavelengths and comparing them with the predictions for a pulsating blackbody without limb darkening, we can estimate the limb-darkening coefficients β_λ and, hence, derive information about the temperature structure of the atmosphere.

1.2. *HR 3831: Simple is Better*

The bright (V = 6.17) roAp star HR 3831 (HD 83368), the most extensively studied of the entire class, is an ideal candidate for such an analysis. Usually, the diagnostic value of a roAp star is enhanced by having a rich eigenfrequency spectrum with many excited modes and overtones, offering the best opportunity to apply asymptotic p-mode theory to the data. However, in this case, it is the simplicity of HR 3831 which is its greatest virtue.

This star's eigenfrequency spectrum appears to be dominated by a dipole mode with a period near 11.8 minutes (see Kurtz, Kanaan, & Martinez 1993). Although the frequency spectrum of this mode is split into as many as seven closely spaced components (due to the combined perturbations of the magnetic field and rotation; (Kurtz 1992), there is no evidence for other independently excited p-modes (as seen in several roAp stars; e.g., Kurtz et al. 1989; Matthews, Kurtz, & Wehlau 1987) which would produce beating effects and make it difficult to interpret the observed amplitudes.

The amplitude and phase of the dipole mode is modulated with the period of magnetic variations, which is taken to be the star's rotation period ($P_{\rm rot} \simeq 2.85$ days). The maximum amplitude in the Johnson B filter is just above 0.004 mag—one of the largest in the sample of known roAp stars and another attractive feature of HR 3831 for our work. Since our limb-darkening analysis is most effective with a long wavelength baseline extending into the near infrared, where the oscillations are expected to be very small, we would like a star with the largest amplitude possible.

Kurtz (1992) has obtained excellent fits to the amplitude and phase changes by adopting the oblique pulsator model, where the pulsation pole of the distorted dipole (l, m) = (1, 0) mode is located near the magnetic pole, and we see different aspects of the nonradial geometry as the star rotates. There is a well-defined ephemeris for times of maximum oscillation amplitude (Kurtz et al. 1993):

$$\mathrm{JD}_{\rm max} = 2{,}448{,}312.24019 + (2.851982 \pm 0.000005)E\,. \qquad (2)$$

Note that HR 3831 undergoes polarity reversal, so both magnetic (and, hence, pulsation) poles appear during the rotation period. Thus, there are oscillation amplitude maxima twice per cycle, at phases 0.0 and 0.5 in the above ephemeris. The relatively short modulation period (compared to more than a week to years for other roAp stars) and the polarity reversal are an added practical bonus, allowing one to catch at least one phase of maximum oscillation amplitude even during a short observing run on a large telescope.

To apply our technique, one must assume the orientation of the dipole mode at the time of observations. The ephemeris is an important part of the determination, but there must be other independent constraints on the nonradial geometry of the star. Fortuntely, HR 3831 obliges in these respects as well. It just happens to be a member of visual binary with a solar-type companion, which Kurtz et al.

[3] Except for the case of $i_{\rm puls} = 90°$, where the two hemispheres of the dipole mode—which vary in antiphase to each other—contribute equally on the visible disk and the net amplitude is zero.

TABLE 1

OBSERVED AMPLITUDE RATIOS OF HR 3831 AS A FUNCTION OF BANDPASS

Filter	Central λ (Å)	FWHM (Å)	Amplitude (mag)	Amplitude Ratio
v.....	4110	190	0.00373	1.00
b	4650	190	0.00340	0.91
y	5500	240	0.00241	0.65
R.....	7000	2200	0.00115	0.31
I.....	8800	2400	0.00144	0.39
J	12500	3800	0.00110	0.29
H.....	16800	3800	0.00075	0.20
K.....	22000	4800	0.00063	0.17

(1993) have exploited to derive a radius of $R = 1.9 \pm 0.1\ R_\odot$ for HR 3831. Combined with its measured $v \sin i = 34 \pm 3$ km s^{-1} and rotation period, this sets a strong lower limit on the rotation inclination: $i \geq 38°$. Furthermore, if one assumes the magnetic field is a pure centered dipole, the observed field strength variation in HR 3831 constrains either the rotational inclination i or the magnetic obliquity $\beta_{\rm mag}$, such that i or $\beta_{\rm mag} \geq 62°$. (The magnetic obliquity is the same as the pulsation pole obliquity for an oblique pulsator.) Kurtz (1992) obtained reasonable fits to the amplitude and phase modulation data for $(i, \beta_{\rm mag}) = (85°, 33°)$ and $(70°, 70°)$.

In summary, HR 3831 is a bright, "large-amplitude" (4 mmag!) roAp star, with a single excited dipole mode whose geometry is constrained by several independent factors and whose well-studied rotational modulation occurs over a conveniently short period of less than 3 days. All these factors lend themselves to the limb-darkening analysis we describe in § 3, and led us to choose this star for our first trial.

2. OBSERVING THE PULSATION AMPLITUDES OF HR 3831

Our goal was to obtain a set of pulsation amplitudes across a wide range of wavelengths. For practical reasons and concerns about our ability to predict how the stellar flux would vary with pulsation at wavelengths shortward of the Balmer jump, we chose to concentrate on the optical and near-infrared regions of the spectrum. Simultaneous measurements under comparable observing conditions are essential if we are to compare reliably the amplitudes at different wavelengths. Optimally, this entails two telescopes at the same site, one equipped with an optical detector and the other an IR device.

On the nights of 1991 November 24 and 25 UT, we obtained high-speed photometry of HR 3831 in five optical bandpasses (Strömgren *vby* and Cousins *RI*) using the 1.0 m telescope and automated single channel photometer of the Cerro Tololo Inter-American Observatory (CTIO). An RCA 31034 phototube was the optical detector. At the same time, we monitored HR 3831 in three IR bandpasses (*JHK*) with the CTIO 1.5 m telescope and infrared photometer. These observations were made with the InSb detector and f/30 chopping secondary.

Integration times were ~20 s in the optical and 1 minute in the infrared—both adequate to sample the 11.8 minute pulsation period. Because of the short period, the measurements were necessarily nondifferential; no comparison stars were used for the rapid photometry.[4] The IR observing sequence was star-sky-sky-star; the optical photometry was interspersed with sky measurements roughly every hour. All the photometric data will be made available as part of the AAS CD-Rom Series, Vol. VI.

A clear detection of oscillations was made on the night of November 25 UT, covering phases 0.38–0.45 in the ephemeris of equation (2) (i.e., just before pulsation amplitude maximum). These data span ~3.6 hr or 18 pulsation cycles. Unfortunately, our other night coincided with phases centered around 0.75, corresponding to zero amplitude in the modulation cycle as the pulsational equator crosses the center of the stellar disk. This, combined with slightly poorer observing conditions, led to a null detection on that night. Therefore, we restrict our analysis to the results from the first night.

To estimate the amplitude of the pulsation mode measured in each filter, we generated a Fourier periodogram for each set of photometry, using a routine for unequally spaced time series (see Matthews & Wehlau 1985). Shown in Figure 2 are the Fourier amplitude spectra in the eight bandpasses. The prominent peak visible in the spectra of data obtained at shorter wavelengths occurs near 122 day^{-1} ($\nu \simeq 1.412$ μHz; $P \sim 11.8$ minutes)—the dominant pulsation mode of HR 3831. Note how rapidly the amplitude drops with increasing wavelength, until only upper limits can be established in the infrared—despite a noise level near 0.0005 mag in K.

Pulsation amplitudes were derived from the Fourier spectra of the v, b, y, R, and I data, while upper limits based on the local noise level were obtained for J, H, and K. These were converted into amplitude ratios normalized with respect to the v amplitude; the results are listed in Table 1. It is difficult to assign formal errors to the amplitude estimates; however, if one uses the general noise envelope in the individual Fourier amplitude spectra as a guide, the uncertainties in the amplitude ratios would be $\sim \pm 0.02$.

3. TRANSLATING PULSATION AMPLITUDES INTO ATMOSPHERIC STRUCTURE

3.1. *Limb-Darkening Coefficients*

Consider a star which is pulsating in a normal nonradial mode of degree l, azimuthal order m, and radial overtone n, whose radial displacement $\xi = \delta r/r$ can be described by an eigenfunction of the form

$$\xi_{n,l,m}(r, \Theta, \Phi, t) = A_n(r) Y_l^m(\Theta, \Phi) e^{-2\pi i t/P}, \quad (3)$$

where Y_l^m is the appropriate spherical harmonic, $A_n(r)$ is the amplitude as a function of radius r (which depends on the overtone), and P is the pulsation period. (The coordinates Θ and Φ are the latitude and longitude, respectively, on the stellar surface.) The angular dependence of the variations in other physical quantities (density $\delta\rho/\rho$, pressure $\delta p/p$, and temperature $\delta T/T$) is also defined by equation (3). If the perturbations are small (certainly valid for roAp stars) and adiabatic (such that specific entropy is conserved), then $\delta T/T \propto \delta\rho/\rho \propto \delta\rho/\rho$ (see, e.g., chap. 13 of Unno et al. 1989).

[4] Our experience and that of others (e.g., Kurtz et al. 1989) has shown that the rapid oscillations of roAp stars can be reliably detected in such nondifferential data, given only slow variations in the local atmospheric transparency.

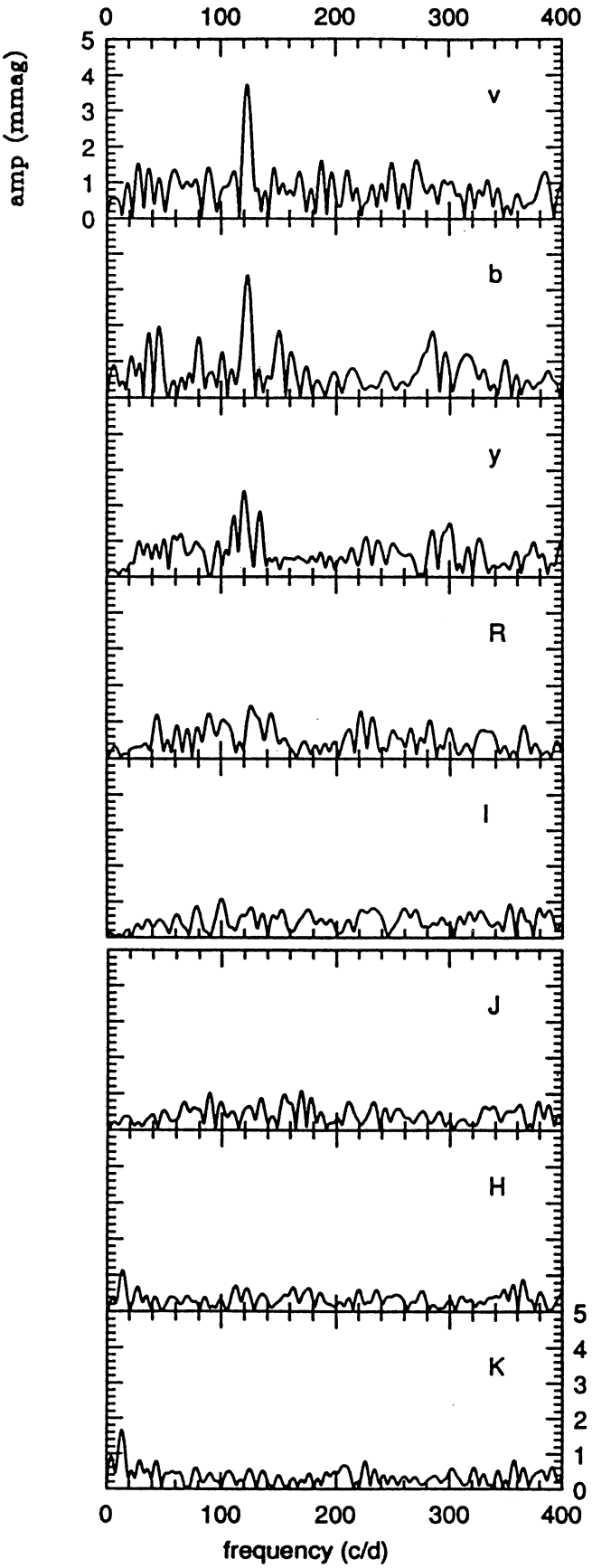

FIG. 2.—Fourier amplitude spectra of the pulsations of HR 3831 in eight bandpasses. The spectra have been oversampled to ensure that the true amplitudes of the Fourier peaks are obtained; the Nyquist frequency for the IR data is over 700 day^{-1} and for the optical data it is about 3 times higher.

For our approach, we assume that the *intrinsic* luminosity variations of the star are those of an oscillating blackbody whose effective temperature variations at each point on the stellar surface are regulated by equation (3). To compute the ratio of expected pulsation amplitudes for a given mode integrated across the stellar disk with and without limb darkening, the time- and overtone-dependent terms can be neglected, leaving the angular dependence of Y_l^m.

To simulate the brightness oscillations of an $(l, m) = (1, 0)$ mode whose pulsation pole is tipped by some inclination $i_{\rm puls}$ to the observer, we sample the visible hemisphere of the star with a grid in latitude Θ and longitude Φ. The grid has pixels of equal surface area whose contributions to the visible disk are weighted by their projected area in the plane of the sky. Typical grids contain almost 130,000 pixels. Because the total disk area of a star pulsating in a dipole mode remains constant, we can attribute all the intrinsic luminosity variations in the star to changes in its effective temperature.[5] With a mean effective temperature $T_{\rm eff}$, maximum temperature variation $\Delta T_{\rm puls}$, and pulsation pole inclination $i_{\rm puls}$ as input, the local range of temperature variation within each pixel on the grid is normalized according to equation (3) for a dipole mode. The local range of flux variation in each pixel is obtained from the Planck function at minimum and maximum temperature, convolved in wavelength with the response function of the desired filter bandpass. Finally, the results are integrated across the visible disk to produce to produce the photometric amplitude of the mode, which would be measured in the *absence* of limb darkening.

The effects of limb darkening on the net observed amplitude are included by repeating the above calculations, but now applying to each pixel on the simulated disk an angular weighting term defined by equation (1), where the limb-darkening coefficient β_λ is an input parameter. In this way, for a selected bandpass, one can produce a ratio $A_{\rm obs}/A_{\rm int}$ of the observed limb-darkened amplitude over the intrinsic undarkened amplitude (or alternatively, an amplitude ratio for two different choices of β_λ).

For a set of observed amplitudes obtained simultaneously through different filters, we have a corresponding set of amplitude ratios normalized with respect to one of the bandpasses. Then we run our model iteratively to perform a least-squares fit of the observed amplitude ratios versus wavelength, where the wavelengths are the central wavelengths of the bandpasses and the values of β_λ are free parameters. Because the model produces only *relative* amplitudes, we must constrain the least-squares solution in one of two ways: (1) assume an analytical form for the dependence of β_λ on λ; e.g., a power-law relation (which is a good approximation to solar limb darkening over the optical and near-IR infrared wavelength range), or (2) fix the value of β_λ for a selected bandpass and allow the other values to be fitted freely. The end result is a set of limb-darkening coefficients for the central wavelengths of the filters used.

[5] Note that even *local* radius variations must be very small. Measurements of the radial velocity oscillations of roAp stars by Matthews et al. (1988), Libbrecht (1988), and Scott & Matthews (1995) find disk-integrated amplitudes of less than 300 m s^{-1}. Over the ~12 minute period of HR 3831, this represents an average radial excursion of less than 70 km, or $\delta R/R \simeq 5 \times 10^{-5}$ for a 2 $R_\odot$ star.

3.2. *The Source Function*

Armed with a set of coefficients β_λ, we can now substitute equation (1) in the transfer equation:

$$\frac{I_\lambda(\theta)}{I_\lambda(0)} = \int_0^\infty \frac{S_\lambda(\tau_\lambda)}{I_\lambda(0)} e^{-\tau_\lambda \sec\theta} \sec\theta \, dr_\lambda , \quad (4)$$

where $I_\lambda(0)$ is the emergent intensity at the subsolar point on the disk at wavelength λ, τ_λ is the optical depth at that wavelength, and the source function S_λ is treated as the expansion

$$S_\lambda(\tau_\lambda) = a_0 + a_1\tau_\lambda + a_2\tau_\lambda^2 + a_3\tau_\lambda^3 + a_4\tau_\lambda^4 + a_5\tau_\lambda^5 + \cdots . \quad (5)$$

To solve equation (4), we have two options for dealing with the source function $S_\lambda(\tau_\lambda)$: (1) solve for the coefficients a_j by inversion of a $j \times j$ matrix for specific values of θ across the stellar disk; or (2) adopt the Eddington-Barbier relation (Barbier 1943); i.e., truncate equation (5) to include only two terms $S_\lambda(\tau_\lambda) = a_0 + a_1\tau_\lambda$. Finally, the resulting expression for the source function is equated with the Planck function,

$$S_\lambda(\tau_\lambda) = \frac{2hc^2}{\lambda^5} \frac{1}{e^{hc/\lambda kT} - 1} , \quad (6)$$

assuming a blackbody dependence to produce the temperature structure as a function of optical depth. This is essentially the same approach as is used to derive the T-τ curve for the Sun's photosphere.

4. A SEMIEMPIRICAL T-τ RELATION FOR HR 3831

4.1. *Model Input Parameters*

The input parameters for the fitting procedure described in § 3.1 to derive limb-darkening coefficients β_λ are: (1) the star's mean effective temperature $T_{\rm eff}$, (2) the maximum range of photospheric temperature variation due to pulsation $\Delta T_{\rm puls}$, and (3) the inclination of the pulsation pole $i_{\rm puls}$ at the time of the measurements.

Kurtz et al. (1993) estimate the mean temperature of HR 3831 to be $T_{\rm eff} \simeq 8000$ K, based on its Strömgren β index and the calibration of Moon & Dworetsky (1985). Adelman et al. (1995) warn that the temperatures of Ap stars may be overestimated by this technique. Therefore, we conducted tests with temperatures in the range 7000 K $\leq T_{\rm eff} \leq$ 8500 K. Since the maximum range in light variation during the oscillation cyle of HR 3831 is less than 1%, and none of that should be due to changes in the stellar surface area, we can set an upper limit to the change in effective temperature (averaged over the stellar surface) defined by the relation

$$\frac{\delta L}{L} = \frac{\delta F}{F} = 4 \frac{\delta T_{\rm eff}}{T_{\rm eff}} , \quad (7)$$

where L is the stellar luminosity and F the flux. Thus, we expect $\Delta T_{\rm eff}/T_{\rm eff} \leq 0.0025$, so that $\Delta T_{\rm eff} \leq 20$ K. To be conservative, tests were conducted with $10 \leq \Delta T_{\rm puls} \leq 60$ K. The final results proved quite insensitive to the exact values of $T_{\rm eff}$ and $\Delta T_{\rm puls}$.

Model fits were performed for a range of inclinations of the pulsation pole, $30° \leq i_{\rm puls} \leq 80°$. The lower bound on $i_{\rm puls}$ is set by the phase of the observations in the magnetic cycle of HR 3831; at phase 0.4, the magnetic pole (= pulsation pole) can be no closer to the subsolar point than $\sim 30°$ (since it must pass across the star's meridian at phase 0.5). The upper bound cannot be too close to 90°, since, at such high inclinations, the amplitude of the (l, m) = (1, 0) mode would be almost zero. As it turned out, for $i \geq 65°$, the model amplitude ratios could never reproduce the observations regardless of the choice of other parameters, so our technique may also set additional constraints on the geometry of HR 3831.

As mentioned in § 1.2, Kurtz (1992) obtained good agreement with the modulation data for HR 3831 using (i, $\beta_{\rm mag}$) = (85°, 33°) and (70°, 70°). These sets of parameters translate into $i_{\rm puls}$ values of $\sim 50°$ and 30°, respectively, at phase 0.4. Looking back at Figure 1, one can see that the amplitude enhancement by limb darkening is relatively insensitive to the inclination of the pulsation pole for $0° \leq i_{\rm puls} \leq 50°$. Based on the above considerations, we finally adopted $i_{\rm puls} \simeq 40°$.

To solve equation (5), we must assume a value for $I_\lambda(0)$, the emergent intensity from the subsolar point on the stellar disk. Kurtz et al. (1993) use photometric indices and the binary companion to HR 3831 to conclude that the star is of type A7 V and lies 0.7 mag above the zero-age main sequence, with a mean temperature of 8000 K. For this temperature, we calculate a central intensity at $\lambda = 5000$ Å of $I_\lambda(0) \simeq (1.07^{+0.26}_{-0.23}) \times 10^7$ ergs cm^{-2} s^{-1} Å, where the errors correspond to a conservative uncertainty in temperature of ± 500 K.

4.2. *Limb-Darkening Coefficients*

The limb-darkened models were fitted to the observed amplitude ratios in Table 1 to minimize the total χ^2 for the eight bandpasses. Because the models do not produce *absolute* amplitudes in each bandpass, it is necessary to constrain the fit as described in § 3.1. We tried two simple options.

First, we forced a power-law relation for the limb-darkening coefficients as a function of wavelength

$$\log \beta_\lambda = A \log \lambda + B , \quad (8)$$

where A and B are free parameters. Such a relation is a good description of limb darkening on the Sun over the wavelength range of our observations. The best fit to the data is shown in Figure 3*a*, along with the corresponding curve for solar limb darkening. Our fit yields a power-law slope of $A = -1.44 \pm 0.01$ and a zero point of $B = 5.20 \pm 0.02$; the corresponding solar values are $A_\odot \simeq -0.7$ and $B_\odot \simeq 3.5$. Note how solar limb darkening results in amplitudes larger than observed at all wavelengths above 4110 Å. However, while our best fit to equation (8) does depress the amplitudes at longer wavelengths, it still does not reach the upper limits set by the infrared data. Note also that the observed R amplitude is too low for a monotonic decrease in amplitude with wavelength, which is the only type of trend possible from a monotonic β_λ versus λ relation like equation (8).

Therefore, as a second approach, we fixed the value of β_λ for a chosen bandpass and allowed the other seven values to vary freely. We first tried low values for the K coefficient, dropping as low as $\beta_{\lambda=2.2\,\mu} = 0$, then high values for the v coefficient, as high as $\beta_{\lambda=4110\,\text{Å}} = 1$. Our best fit is plotted in Figure 3*b*, in which the observed amplitude ratios and limits appear to be well reproduced.

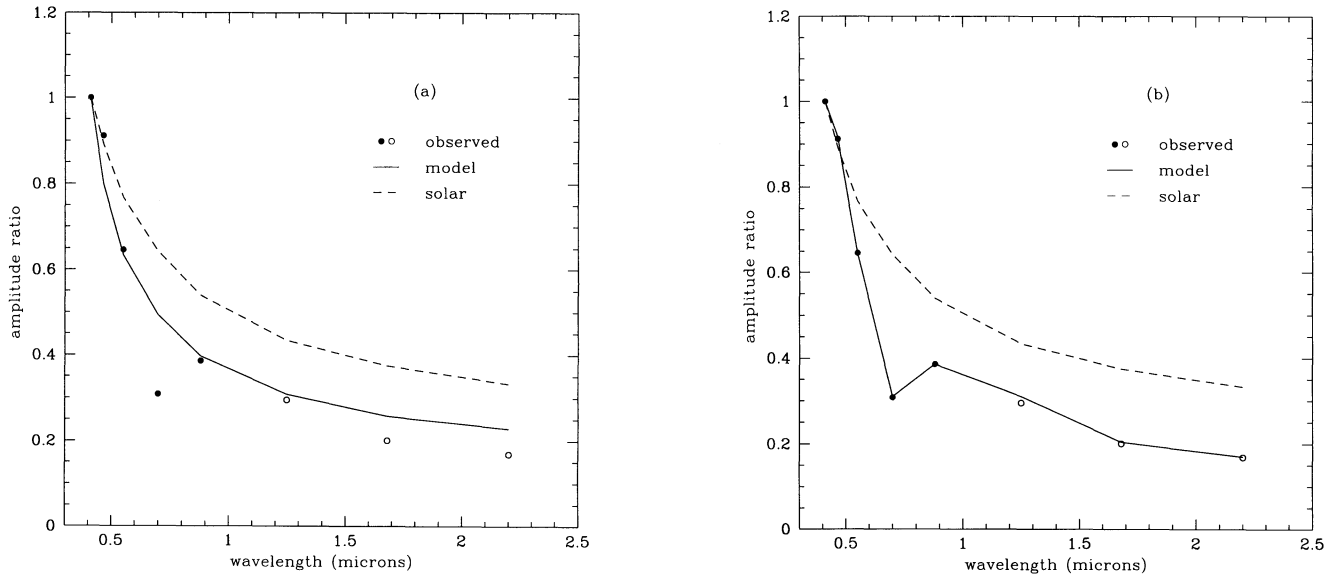

FIG. 3.—Three fits to the observed pulsation amplitude ratios (*filled circles*) and upper limits (*open circles*) with different restrictions on β_λ. The mean temperature in all cases is 8000 K. The dashed line in each panel is the prediction based on solar limb-darkening coefficients. (*a*) A power-law fit of β_λ vs. λ. (*b*) The coefficient is fixed at $\lambda = 4110$ Å, the other values are allowed to float freely.

Values of β_λ for each bandpass are listed in Table 2, corresponding to the Sun, our power-law model (case *a*), and our free-fitting solution (case *b*). In both fits, the data call for a much steeper dependence of limb darkening on wavelength than applies in the Sun's photosphere. We adopt the values from column (4) of Table 2 as the optimum fit.

4.3. *Temperature versus Optical Depth*

At first, to solve equation (5), we assumed a six-term expansion of the source function $S_\lambda(\tau_\lambda)$ and carried out a 6×6 matrix inversion (Press et al. 1991) to obtain the coefficients a_i in equation (6). When this expansion of the source function was substituted in equation (7), the resulting T versus τ_{5000} curve contained a strong temperature inversion around log τ_{5000} curve contained a strong temperature inversion around log $\tau_{5000} \sim 0.7$. This preliminary result was reported by Matthews et al. (1993a, b).

However, after considering the actual number of degrees of freedom represented by our data and taking our cue from limb-darkening analyses of the Sun, we realized that a six-term fit to $S_\lambda(\tau_\lambda)$ overinterprets the available data. In the case of the Sun, where the limb-darkening curve can be measured explicitly on the disk, no more than three coefficients in the expansion of equation (6) can be obtained reliably via this approach—even where the data have an accuracy of $\pm 1\%$ (e.g., Böhm 1961). Adding more terms to the fit can reproduce the solar limb darkening but generates wild fluctuations in the solution of $S_\lambda(\tau_\lambda)$.

To be conservative, we have instead adopted the Eddington-Barbier relation (Barbier 1943) and assumed that the source function has a linear dependence on optical depth: $S_\lambda(\tau_\lambda) = a_0 + a_1\tau_\lambda$, where a_0 and a_1 are free parameters in the solution.

Because we specify a linear relation, we glean little information about the true *shape* of the atmospheric temperature gradient, but we do recover robust information about its mean slope within the protosphere. The largest optical depth to which we are sensitive is $\tau_\lambda \sim 1$, whereas the lower limit is less well defined. In the solar case, the angular resolution at the limb attributable to seeing sets a limit on the minimum depth of $\sim 10^{-3}\ R_\odot$ that can be resolved in the photosphere. Since our technique relies on photometric amplitude measurements integrated over the entire stellar disk, it is more difficult for us to specify a lower limit on optical depth. We have chosen to present the range $0 \geq \log \tau_\lambda \geq -3$.

The resulting temperature versus optical depth curve at $\lambda = 5000$ Å is tabulated in Table 3 and plotted in Figure 4 (*solid line*). Also shown in Figure 4 are the standard solar curve (*long-dashed line*) and two theoretical T-τ_{5000} relations relevant to Ap stars, which are discussed below.

TABLE 2

FITS TO THE LIMB-DARKENING COEFFICIENTS β_λ OF HR 3831

Wavelength (Å) (1)	Solar Value (2)	Case *a* (3)	Case *b* (4)
4110	0.85	0.99	0.98
4650	0.80	0.83	0.93
5500	0.70	0.65	0.56
7000	0.58	0.46	0.04
8800	0.48	0.33	0.11
12500	0.40	0.20	0.07
16800	0.34	0.13	0.05
22000	0.29	0.09	0.02

5. CONCLUSIONS, CAVEATS, AND CONTINUED EFFORTS

5.1. *Comparison with Gray and Model Atmospheres*

Figure 4 reveals that the temperature gradient in HR 3831 is substantially steeper than that for the Sun. As a result, the surface temperature of HR 3831 is cooler than one would infer from its effective temperature, assuming a standard gray atmosphere.

Such a situation had already been suggested by Shibahashi & Saio (1985) to explain how some roAp stars could pulsate with frequencies above the acoustic cutoff for a gray atmosphere. They noted that if the atmospheric temperature gradient were steeper, then the cutoff frequency

TABLE 3

A SEMIEMPIRICAL T-τ_{5000} RELATION FOR HR 3831

log τ_{5000}	T (K)	log τ_{5000}	T (K)	log τ_{5000}	T (K)
0.000.....	8626.4	−1.000.....	6463.9	−2.000.....	6146.7
−0.050.....	8412.7	−1.050.....	6427.7	−2.050.....	6142.6
−0.100.....	8215.5	−1.100.....	6394.9	−2.100.....	6139.0
−0.150.....	8033.6	−1.150.....	6365.4	−2.150.....	6135.7
−0.200.....	7865.8	−1.200.....	6338.7	−2.200.....	6132.8
−0.250.....	7711.1	−1.250.....	6314.8	−2.250.....	6130.2
−0.300.....	7568.5	−1.300.....	6293.2	−2.300.....	6127.8
−0.350.....	7437.2	−1.350.....	6273.8	−2.350.....	6125.8
−0.400.....	7316.4	−1.400.....	6256.4	−2.400.....	6123.9
−0.450.....	7205.5	−1.450.....	6240.8	−2.450.....	6122.3
−0.500.....	7103.6	−1.500.....	6226.8	−2.500.....	6120.8
−0.550.....	7010.2	−1.550.....	6214.2	−2.550.....	6119.5
−0.600.....	6924.7	−1.600.....	6203.0	−2.600.....	6118.3
−0.650.....	6846.6	−1.650.....	6192.9	−2.650.....	6117.3
−0.700.....	6775.2	−1.700.....	6183.9	−2.700.....	6116.4
−0.750.....	6710.2	−1.750.....	6175.9	−2.750.....	6115.5
−0.800.....	6651.0	−1.800.....	6168.6	−2.800.....	6114.8
−0.850.....	6597.2	−1.850.....	6162.2	−2.850.....	6114.1
−0.900.....	6548.3	−1.900.....	6156.4	−2.900.....	6113.5
−0.950.....	6504.0	−1.950.....	6151.3	−2.950.....	6113.0

would be raised. Shown as the dotted line in Figure 4 is one of the T-τ relations (their "model B") consistent with the highest frequency seen in the roAp star HR 1217. The shape of their curve is different, since they adopted a different analytical form (although we note that their model series A and C were based on the Eddington approximation and also satisfied the acoustic cutoff criterion). However, the mean T-τ gradient is very similar for their model and our result.

Recently, Muthsam & Stepień (1992) published sets of Ap model atmospheres for three different chemical compositions and a range of effective temperatures. Although their models do contain a somewhat artificially constructed line opacity, and the authors themselves admit that their grid is rather limited, they have succeeded in fitting the line profiles of several Ap stars at different rotational phases. Furthermore, the authors do provide tables of the atmospheric structures of their models which we can use to compare with our results. The short-dashed curve in Figure 4 is their tabulation of T versus Rosseland optical depth for $T_{\rm eff}$ = 8000 K, log g = 3.5, and a pseudomicroturbulence meant to represent a magnetic field of 1000 G. This curve is very similar to the Shibahashi & Saio (1985) solution and, again, is consistent with the steep gradient we find for HR 3831.

A gradient steeper than solar is also what we would intuitively expect, given the anomalous concentrations of certain heavy elements in the upper atmospheres of Ap stars. These enhanced levels of rare earths and Fe-peak ions (presumably caused by chemical diffusion) provide extra opacity higher in the photosphere. As an aside, we note that abundance measurements based on equivalent widths assuming gray atmospheric structure may have systematic errors. Our observational evidence for a nongray atmosphere with a measured temperature gradient should make possible more self-consistent abundance estimates.

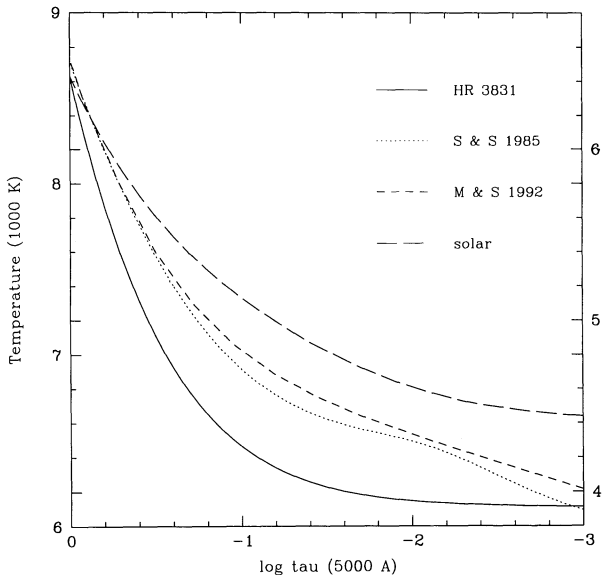

FIG. 4.—Temperature gradient in the photosphere of HR 3831 (*solid line*) compared to the Sun (*long-dashed line*) and two theoretical curves suggested for Ap stars: the Shibahashi & Saio (1985) model (*dotted line*) and the Muthsam & Stepień (1992) model (*dashed line*). Temperature scale for the solar curve is shown on the right-hand axis; it was shifted vertically so that the temperature curves of the Sun and HR 3831 would intersect at τ_{5000} = 1. The model curves have *not* been shifted relative to our result.

5.2. *An Opacity Diagnostic*

It may be possible to extract from our results some information about the dominant sources of opacity in an Ap atmosphere, in a way similar to that applied to the Sun. (See Zirin 1988, chap. 6, for a review of the solar results.)

We can define the optical depth τ_λ according to the following relation:

$$d\tau_\lambda = -k_\lambda \rho \, dx \, , \tag{9}$$

where k_λ is the absorption coefficient, ρ is the density, and x is a geometrical depth. If we differentiate this equation with respect to temperature, we obtain

$$\frac{d\tau_\lambda}{dT} = -k_\lambda \rho \frac{dx}{dT} \, . \tag{10}$$

The derivative on the left-hand side of this equation can be

obtained from our T-τ_λ solution. Since the derivative on the right-hand side, dx/dT (relating temperature to *geometrical* depth), is independent of wavelength, we can use equation (10) to determine the wavelength dependence of the opacity at a given temperature in the atmosphere. For fixed T,

$$\frac{dT}{d\tau_\lambda} \propto \frac{1}{k_\lambda \rho} . \tag{11}$$

Pierce & Waddell (1961) were able to compare solar measurements of $dT/d\tau_\lambda$ as a function of wavelength with theoretical values for H^- absorption. The excellent agreement at different temperatures in the photosphere firmly established the negative hydrogen ion as the principal source of continuous opacity in the Sun.

In Figure 5 we show the dependence of log $(dT/d\tau_\lambda)$ on λ at a temperature of $T = 6300$ K, based on our solution of T versus τ_λ for the eight bandpasses sampled in HR 3831. Also shown for comparison is the prediction for H^- continuous opacity at the same temperature. Clearly the points and the curve do not agree. This could be telling us that H^- is not the only strong continuous opacity source in an Ap atmosphere. However, it will be necessary to compare these results with theoretical predictions for other candidate opacity sources before drawing any firm conclusions.

5.3. *Caveats*

Keep in mind that our results are valid only for one rotational phase of HR 3831, just before magnetic maximum. The extreme atmospheric properties inferred here—close to the magnetic pole—may differ from the average over the entire surface of the star. (Although we have some data for HR 3831 from a second night, the amplitudes are beneath reliable detection limits, as expected from the modulation phase of the star at that time; see § 2.) Accurate multicolor photometry at a full range of rotational phases will be necessary to investigate the horizontal variations in atmospheric structure.

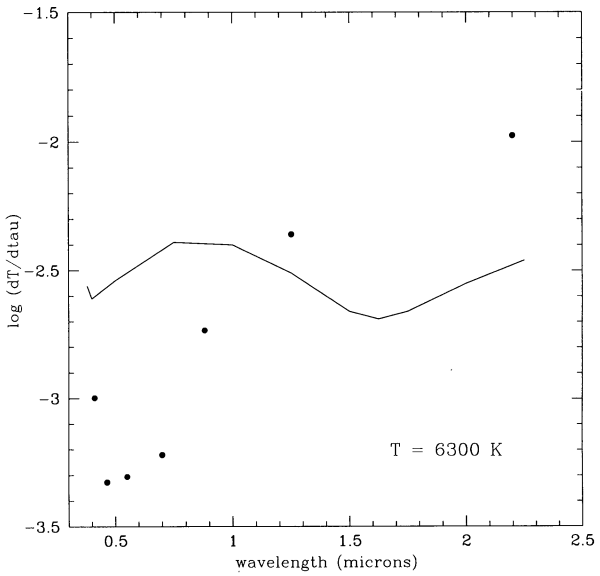

FIG. 5.—Wavelength dependence of the opacity derived from the atmospheric structure we find for HR 3831 (*filled circles*) compared to theoretical predictions for H^{-1} continuous opacity (*solid curve*) from Pierce & Waddell (1961).

Horizontal gradients in the atmospheric properties may also present another problem. We have assumed that the dependence of observed amplitude on wavelength is due entirely to the weighting of a blackbody source by limb darkening. This may not be the whole story; flux redistribution by photospheric spots is another possible contributor. Indeed, temperature and abundance maps of the surfaces of several Ap stars generated through Doppler imaging (e.g., Rice & Wehlau 1991) indicate the presence of spots and rings associated with the magnetic field geometry. Although these patterns may evolve very slowly, over short timescales they should be essentially locked into the same orientation with the magnetic dipole axis and, hence, the pulsation mode axis. A Dopper image of HR 3831 would allow us to include the effects of this temperature distribution on the mode. In fact, because the limb darkening on the disk would not change during rotation in the same way as any atmospheric pattern fixed to the stellar surface, a set of multicolor photometry well sampled in rotational phase might be able to segregate the two effects, even without independent mapping information.

Even so, significant flux redistribution out to infrared wavelengths of 2.2 μm seems unlikely, so it is still difficult to avoid the steep T-τ curve we find for HR 3831, if we are to account for its pulsation amplitudes.

Have we properly described the intrinsic pulsational variations of HR 3831 and their angular dependence across the stellar disk? Kurtz (1992) argues that the nonradial mode of HR 3831 cannot be treated simply as a pure spherical harmonic mode if one is to reproduce the observed amplitude and phase modulation: Instead, he describes the mode of HR 3831 as a "distorted dipole" whose dominant form is dipolar. We did consider adding the additional harmonic terms fitted by Kurtz (1992); however, the amplitude and phase modulation of the mode will be affected by the limb darkening as well, since the pulsation pole changes its observed inclination during rotation. This effect is particularly pronounced at high inclinations (see Fig. 1), and Kurtz's fits do not include it, since it was not recognized at that time. Therefore, we are awaiting new harmonic fits before we pursue this possibility further.

Another concern is our reliance on equation (1) to describe the limb darkening. We have no choice but to assume a simple analytical form which contains only one free parameter if we wish to perform a meaningful inversion. While equation (1) is a reasonable (but far from perfect) approximation for the Sun and is widely applied to other stars (in the absence of any data to test it), the true form of limb darkening in Ap stars is probably somewhat more complicated. Eventually, our technique could be used in the opposite sense to what we have done in this paper. Rather than "inverting" the amplitude data into a simple set of coefficients, one might try a "forward" approach: A trial model atmosphere for an Ap star could be used to predict pulsation amplitudes as a function of wavelength. The results would be compared to observation, and the process repeated iteratively until the best match is found.

5.4. *What Next?*

One of the limitations in our current analysis is that we were unable to detect the oscillations of HR 3831 at infrared wavelengths, having to setting for upper limits on the *JHK* amplitudes. The anticipated low amplitudes make such detections a challenge from the ground (see, e.g., Weiss et al.

1991; Belmonte, Martínez, & Roca Cortés 1991). The best results would be obtained from an orbiting infrared observatory like the *Infrared Space Observatory* (*ISO*).

In the meantime, however, there are still clear priorities for ground-based photometric campaigns. A new campaign on HR 3831 would be appropriate, to obtain better phase coverage of the rotation cycle and lower noise levels in the IR. Also, since our original measurements, another prime candidate for our technique has emerged: α Circini (HR 5463 = HD 128898). This is the brightest of the known roAp stars ($V = 3.19$), with a pulsation period near 6.8 minutes. However, there were no clear indications of its rotation period or the geometry of its pulsation mode until Kurtz et al. (1994) identified a rotational split triplet in the frequency pattern of its dominant dipole mode and measured its amplitude modulation period. As a result, the rotation period of α Cir is now known to be $P_{\rm rot} = 4.4790 \pm 0.0001$ days. Kurtz et al. (1994) further provide a table of constraints on the rotational inclination and obliquity of the mode. One drawback for this star is the presence of other closely spaced p-modes, but their amplitudes are very low relative to the principle dipole mode. Therefore, for the same reasons given in § 1.2, α Cir is now another attractive target for limb-darkening analysis.

On the topic of other candidates for our technique, we point out that, in principle, this analysis could be applied to *any* nonradially pulsating star dominated by a dipole mode. This may prove relevant to some of the nonradial δ Scuti stars, if the modes can be identified unambiguously.

In a similar vein, we note that Heynderickx (1991) independently applied the weighting effect of limb darkening to interpret the pulsations of β Cephei stars. However, his goal was opposite to ours. In order to identify the unknown modes in several multiperiodic β Cephei stars, he adopted a parameterized limb-darkening function and pulsation model to predict their amplitudes. He then used the observed amplitudes to assign a nonradial degree to each frequency. While Heynderickx assumes an atmospheric structure to act as a mode discriminant in the absence of a theoretical eigenmode spectrum for each star, we have chosen a star whose mode is already known and use it to infer its atmospheric structure. Both applications are good examples of the critical role that limb darkening must play in the interpretation of stellar pulsations at different wavelengths.

6. SUMMARY

The observed pulsation amplitudes (and upper limits) of HR 3831 as a function of wavelength indicate a steeper T-τ relation than for the solar atmosphere, agreeing with the acoustic cutoff arguments of Shibahashi & Saio (1985) and the synthetic spectra of Muthsam & Stepień (1992) (see Fig. 4).

We find that the wavelength dependence of the gradient $dT/d\tau_\lambda$ for fixed temperatures does not agree with expectations for H^- continuous opacity, which may indicate that other capacity sources are most important in this star.

These results apply only to the hemisphere of HR 3831 seen when one of the magnetic poles dominates the disk. Our procedure should be repeated at various rotational phases to probe horizontal gradients in atmospheric structure. The results may also be influenced by flux redistribution attributable to spots on the stellar surface. Doppler imaging of HR 3831 (which is feasible given its projected rotation of $v \sin i \simeq 34$ km s^{-1}) would produce a surface temperature map to allow us to account for this effect.

We caution that limb darkening must play some role in the rotational modulation of roAp oscillations, since the observed aspect of the dipole mode changes with time and the enhancement effect of limb darkening varies with mode aspect (Fig. 1). This may change the published harmonic solutions of the distorted dipole of HR 3831 (Kurtz 1992; Kurtz et al. 1993), which are necessary to properly interpret the Coriolis and magnetic perturbations on the star's pulsations (Dziembowski & Goode 1995).

Finally, we identify another strong candidate for limb-darkening analysis—the bright roAp star α Circini—and emphasize that our technique could be applied to any star pulsating in a dominant $(l, m) = (1, 0)$ mode, not only roAp stars.

We would like to thank Chuck Cowley, Don Kurtz, Hiromoto Shibahashi, Tobias Kreidl, and Werner Weiss for useful discussions, as well as the Director and technical staff of CTIO for their support of our observing run. We are also grateful for referee Saul Adelman's useful comments. This work has been funded by research grants to all four authors by the Natural Sciences and Engineering Research Council (NSERC), Canada.

REFERENCES

Adelman, S. J., Pyper, D. M., Lopez-Garcia, Z., & Caliskan, H. 1995, A&A, 296, 467
Barbier, D. 1943, Ann. d'Astrophys., 6, 113
Belmonte, J. A., Martínez R. C., & Roca Cortés, T. 1991, A&A, 248, 541
Böhm, K.-H. 1961, ApJ, 134, 264
Heynderickx, D. 1991, Ph.D. thesis, Katholieke Universiteit Leuven
Kurtz, D. W. 1982, MNRAS, 200, 807
———. 1990, ARA&A, 28, 607
———. 1992, MNRAS, 259, 701
Kurtz, D. W., Kanaan, A., & Martinez, P. 1993, MNRAS, 260, 343
Kurtz, D. W., et al. 1989, MNRAS, 240, 881
Kurtz, D. W., Sullivan, D. J., Martinez, P., & Tripe, P. 1994, MNRAS, 270, 674
Kururz, R. 1993, in ASP Conf. Ser. 44, Peculiar vs. Normal Phenomena in A-Type and Related Stars, ed. M. Dworetsky, F. Castelli, & R. Faraggiana (San Francisco: ASP), 87
Libbrecht, K. 1988, ApJ, 330, L51
Martinez, P., & Kurtz, D. W. 1995, in ASP Conf. Ser. 83, The Astrophysical Applications of Pulsating Variable Stars, ed. R. M. Stobie & P. Whitelock (San Francisco: ASP), 58
Matthews, J. M. 1993a, in ASP Conf. Ser. 42, GONG 1992: Seismic Investigation of the Sun and Stars, ed. T. M. Brown (San Francisco: ASP), 303
———. 1993b, in New Perspectives on Stellar Pulsation and Pulsating Variable Stars, ed. J. M. Nemec & J. M. Matthews (Cambridge: Cambridge Univ. Press), 122
Matthews, J. M., Kurtz, D. W., & Wehlau, W. H. 1987, ApJ, 313, 782
Matthews, J. M., & Wehlau, W. H. 1985, PASP, 97, 841
Matthews, J. M., Wehlau, W. H., Rice, J., & Walker, G. A. H. 1993a, in ASP Conf. Ser. 40, Inside the Stars, ed. W. W. Weiss & A. Baglin (San Francisco: ASP), 199
———. 1993b, in ASP Conf. Ser. 44, Peculiar vs. Normal Phenomena in A-Type and Related Stars, ed. M. M. Dworetsky, F. Castelli, & R. Faraggiana (San Francisco: ASP), 87
Matthews, J. M., Wehlau, W. H., & Walker, G. A. H. 1990, ApJ, 365, L81

Matthews, J. M., Wehlau, W. H., Walker, G. A. H., & Yang, S. 1988, ApJ, 324, 1099
Moon, T. T., & Dworetsky, M. M. 1985, MNRAS, 217, 305
Muthsam, H., & Stepień, K. 1992, Acta Astron., 42, 117
Pierce, A. K., & Waddell, J. 1961, MmRAS, 68, 89
Press, W. H., Flannery, B. P., Teukolsky, S. A., & Vetterling, W. T. 1991, Numerical Recipes in C (Cambridge: Cambridge Univ. Press)
Rice, J. B., & Wehlau, W. H. 1991, A&A, 246, 195
Scott, S., & Matthews, J. M. 1995, in preparation
Shibahashi, H., & Saio, H. 1985, PASJ, 37, 245
Unno, W., Osaki, Y., Ando, H., Saio, H., & Shibahashi, H. 1989, Nonradial Oscillations of Stars (2d ed.; Tokyo: Univ. Tokyo Press)
Weiss, W. W., & Schneider, H. 1984, A&A, 135, 148
Weiss, W. W., Schneider, H., Kuschnig, R., & Bouchet, P. 1991, A&A, 245, 145
Zirin, H. 1988, Astrophysics of the Sun (Cambridge: Cambridge Univ. Press)